

Smartphone-Based Wearable Gait Monitoring System Using Wireless Inertial Sensors

<https://doi.org/10.3991/ijoe.v19i08.38781>

Alejandro Astudillo^{1,2,3}, Edna Avella-Rodríguez¹✉, Gloria Arango-Hoyos¹,
Jose Ramirez-Scarpetta¹, Esteban Rosero¹

¹Universidad del Valle, Cali, Colombia

²MECO Research Team, KU Leuven, Belgium

³Flanders Make@KU Leuven, Leuven, Belgium

edna.avella@correounivalle.edu.co

Abstract—This paper presents a wearable virtual reality system with a wireless network of inertial sensors for lower limb monitoring. The system comprises seven sensor nodes sending data wirelessly to a master node. The information is then collected, organized, and sent to a screening device via a serial interface. An application executed either on a smartphone or a personal computer features an avatar which represents the received data and mimics the sensed movements of the patient, providing online feedback during and after the execution of a therapy. The data resulting from the therapy execution can be uploaded to a web server to facilitate the assessment and decision-making by health professionals. A pendulum featuring a rotary optical encoder is used for sensor functional behavior validation. In addition, the orientation angles measured by the proposed system are compared with respect to measurements from the motion analysis software Kinovea. The delay between the patient's body movement and the avatar is 33 *ms*, which is acceptable for visual feedback. This system is portable, inexpensive and enables a patient to complete physical therapy sessions at home or anywhere, with the advantage of enabling visual feedback through an avatar during rehabilitation therapy and allowing the reproduction of a therapy session for further analysis.

Keywords—wearable sensor, body sensor network, smart device, avatar, virtual reality

1 Introduction

Gait analysis is a research field that studies human locomotion and several musculoskeletal disorders affecting the ability to walk. The gait cycle is a pattern of movement that repeats continuously. Through human gait analysis, kinetic and kinematic parameters can be determined, and the gait phase can be detected. Gait analysis results have been used to evaluate athlete performance [1], [2], monitor patient progress in rehabilitation processes [3]–[6], and to diagnose gait pathologies [7]–[10].

Conventional human motion analysis is performed in closed laboratory environments with force plates and multi-camera motion capture systems [11], [12]. These laboratory systems have a high information processing capacity but are costly and complex to operate. They require long patient preparation times, lengthy post-processing, and highly trained personnel. Another significant limitation is that closed environments imply spatial restrictions, which limit access to this technology in routine clinical practices or in places far from urban centers.

Continuous development of new signals that can be measured, and new information processing and transmitting technologies, have facilitated the arrival of new methods for gait analysis. To characterize gait parameters, video game controllers, e.g., Microsoft Kinect, have been adapted based on artificial vision and treadmills [13]. A brain-machine interface based on cortical potentials has been designed to detect the intention to start walking [14]. To detect and monitor symptoms of Parkinson's disease, a smartphone application has been designed to measure contact time and the start of stimulus and response, as well as posture and gait events using a voice recorder, spatial accelerations and x-y strike coordinates [15]. All these developments require high data processing frequency and are only performed in the sagittal plane.

Among recent technologies used to analyze human gait in the anatomical planes, i.e., the sagittal, frontal and transverse planes, inertial sensors have emerged. An inertial sensor is an electronic device consisting of accelerometers, gyroscopes and magnetometers which measure accelerations, velocities, and orientations. Inertial sensors have gained relevance in the area of gait measurement and, since they can be miniaturized, inertial sensors have turned into low-cost microelectromechanical systems (MEMS). The fusion of the data delivered by these sensors enables reliable kinematic data to be obtained for gait analysis [16]–[21].

Communication technologies such as the internet and mobile devices offer ample opportunities to facilitate access to rehabilitation processes at a reduced cost. New developments in tele-rehabilitation and tele-medicine have emerged and their usability, reliability, validity and effectiveness in comparison to traditional methods have been evaluated [22]–[28]. Taking full advantage of the operational potential in smartphones, applications for consultation and guidance as well as for measurement and monitoring have been designed [29]–[34]. Moreover, visual feedback with avatar systems have been developed aiming at making a physical activity or rehabilitation session more enjoyable [35], [36].

In the case of physical therapies aimed to improve functional mobility after an injury or illness, also known as active kinesiotherapy activities, rehabilitation exercise routines are usually performed by patients without continual supervision by specialists and without monitoring equipment or, in fact, simply at home. As a result, physiotherapists do not know whether patients comply with the specified frequency of assigned exercise routines. Additionally, there is no simple way to correct discrepancies in the completion of assigned tasks nor to quantitatively evaluate the success of the rehabilitation process. Physiotherapists and patients do not have instant feedback from the performed activities, preventing them from actively making improvements or corrections.

A considerable amount of research has been conducted around gait analysis. Nevertheless, little research has been dedicated to integrating new, low-cost and ambulatory technologies with visual feedback capabilities to improve patient progress and support physiotherapists' efforts. Therefore, new flexible, accurate and reliable tools for human movement analysis in any environment, equipped with data communication via the internet, are not only convenient but a necessary aid for the analysis of lower limb movement and therapy. The widespread availability of such tools would be a step forward in ambulatory therapy.

This article presents a smartphone-based wearable monitoring system for the lower limbs based on wireless inertial sensors to analyze human gait. A designed smartphone application provides the user with visual feedback on their movement through an avatar and also enables them to observe the kinematic signals of their lower limbs online. The measured signals are also uploaded to a web server and can be downloaded to another smartphone or a personal computer anywhere. A physiotherapist can then monitor and analyze the tasks performed by a patient to assess a patient's progress or modify the exercises assigned. The proposed system can supply information and data from gait rehabilitation sessions to a physiotherapist, quantifying parameters such as acceleration, angular velocity, and angular positions. This supports decision-making, either for the correction of therapy or to determine treatment completion.

This paper is organized as follows: Section 2 describes the presented lower limb monitoring system including inertial sensors and a smartphone, besides illustrating the data flow and the algorithms used to obtain reliable measurements from the raw data sent by the integrated sensor nodes; the sensor validation and evaluation of the designed lower limb monitoring system with an execution session test are presented in Section 3, while concluding remarks are presented in Section 4.

2 Materials and methods

The proposed system consists of seven wearable inertial sensors, which are attached to the patient's lower limbs. These inertial sensors (or nodes) acquire measurements and send data to a master node (acquisition hardware). The master node then sends the information to a smartphone. An application in the smartphone receives and processes the patient's measurements and generates a moving avatar image allowing the patient to observe their own movements and improve their performance on assigned tasks. When a session is finished, the processed information is uploaded to a web server, where the patient and the specialist can access it for further review and analysis. This information can be downloaded to another smartphone or personal computer anywhere. Physiotherapists can use the designed application to check previous sessions of any patient, observing their movements through an avatar and signal plots. These signal plots include accelerations, angular velocities, and angular positions. Such information can be analyzed by a physiotherapist, who is then able to provide feedback to the patient or modify the exercises to be performed. The system overview is presented in Figure 1.

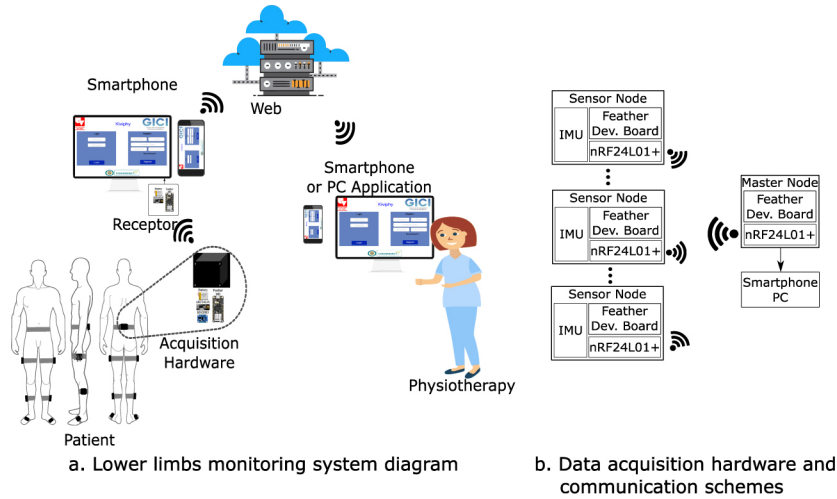


Fig. 1. Data acquisition

2.1 Data acquisition hardware

The data acquisition hardware is based on seven wearable inertial sensor nodes. Each sensor node contains an inertial measurement unit (IMU) equipped with a triaxial accelerometer, a triaxial gyroscope, a triaxial magnetometer sensor, and an integrated microprocessor (BNO055 sensor). It also contains a development board (Feather M0), a wireless radio-frequency communication module (nRF24L01+ from Nordic Semiconductor) and a 3.7 V lithium polymer battery. Using elastic belts, the sensor nodes are fixed on the patient’s lower limbs, as shown in Figure 1a, with a reference sensor node on their pelvis.

A microprocessor at each node executes sensor fusion algorithms and estimates the absolute orientation in Euler angles and quaternions. A development board handles the data acquired from the IMU and sends it to the master node via a wireless radio-frequency communication module with a sampling frequency of 100 Hz. The radio-frequency module is a low-power radio-frequency transceiver able to handle data transfers of up to 2 Mbps through the 2.4 GHz band.

As shown in Figure 1b, the data acquisition hardware is complemented with a master node and a target device (smartphone or personal computer). The master node manages data requests from each of the seven nodes and sends the received data to the target device via a USB interface. The master node has the same components as each of the nodes minus an inertial sensor.

2.2 Software

There are three software applications operating in the wearable virtual reality system for lower limb monitoring presented: an Android application, a PC application, and a web server. Both Android and PC applications are designed and implemented using Unity’s multiplatform gaming engine [37], [38].

Android application. The Android application runs on Android smartphones with an Application Programming Interface (API) level higher than 16. This application’s execution is shown in Figure 2a.



Fig. 2. Graphical user interface of the developed application

The application is divided into three sessions: the user session, the supervision session, and the review session.

In the user session, users can register on the web server or log into the smartphone application using a previously registered username and password. This session is shown in Figure 2a. After logging into the application, if the user is a patient, they will be asked to select the serial port to which the master node is connected. If the user is a physiotherapist, the application lists all patients’ information, and the physiotherapist can decide whether to create a new session or check information from a previous session by running the supervision session or the review session they need.

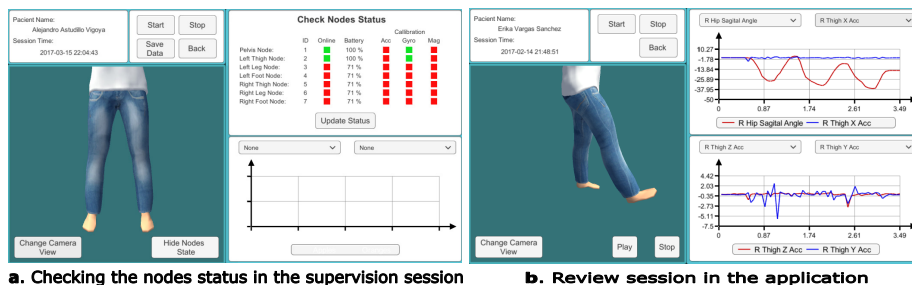


Fig. 3. Sensor status panel and session

The supervision session is the application’s main activity. This session allows the user to acquire information from a patient’s physical activity session. The session plots four acquired signals and displays the avatar representing the patient’s movements.

As can be seen in Figure 2b, the supervision session contains two plots showing two signal red values in each, which each user can freely select. On the left half of the screen, the patient’s name, session date and time, the session control buttons and avatar are displayed. The avatar’s view can be changed from the sagittal plane to a frontal or perspective view. This session also allows the user to check the status of the inertial sensors by checking first if a sensor is online, second if its battery level is sufficient and

third its calibration status. The sensor status panel replaces one of the signal graphs on the screen’s right mid-plane, as shown in Figure 3a. Once the data acquisition is complete, the user can save the retrieved data and upload it to the web server.

Finally, the review session allows the user to check a previously saved session, as shown in Figure 3b. A review session can be executed immediately after a supervision session has ended and the data has been uploaded, or when a physiotherapist needs to examine a previous session. The review session’s display is similar to that of the supervision session. It has a panel to check the status of the inertial sensors and allows the user to play, pause or stop the avatar movement.

Personal computer application. The designed application for Personal Computer (PC) has the same functional features as the smartphone application explained above. While the smartphone application uses Android programming language, the PC application only runs on a Windows-based operating system. The PC application aims to facilitate the physiotherapist’s work and enables them to acquire or visualize information from a patient’s current or previous session. A remarkable advantage of the presented application is its simplicity and ease of use.

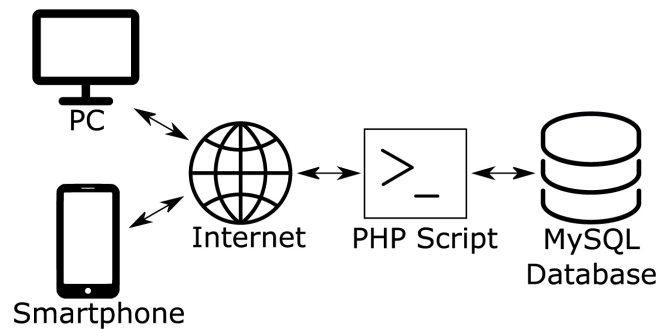


Fig. 4. Web server scheme overview

Web server. User information and data acquired from patients during each physical therapy session are stored on a web server. This web server contains a relational MySQL database and nine PHP scripts that together enable Android and PC applications to interact with the database using web services.

An overview of the web server schema is shown in Figure 4. Both Android and PC applications must connect to the server via internet. However, this connection need not be continuous. These applications establish a connection to the server during user registration, login, data upload and data download.

When a participant of this virtual reality system needs information from the database, the corresponding PC application sends a request to a PHP script hosted on the server. This PHP script sends a query to the MySQL database, processes the response, and delivers a response to the application.

The MySQL database includes two tables: a table of users and a table of therapy sessions. The user’s table includes data such as their name, email, password, and a

Boolean indicating whether or not the user is a physiotherapist. The table of therapy sessions includes the date and time of each session, the respective acquired information, and the username associated with that session.

2.3 Data acquisition and processing

This section explains the data acquisition process performed by the proposed lower limb monitoring system. First, the interaction between the master node and the sensor nodes is explained. Second, the algorithms used to acquire data from the sensors are presented.

Master and sensor nodes interaction. As discussed in Section 2, each of the sensor nodes contains an IMU, a microprocessor and a wireless communication module. The IMU already has a sensor fusion algorithm in place to estimate orientation from raw accelerations, angular velocities and magnetic field strength measurements. All data acquired by the IMUs are stored in multiple registers, one byte per register.

A microprocessor then reads the data registers including the accelerometer, gyroscope, magnetometer, and orientation data represented in the quaternions, as well as the sensor’s calibration information. These data are organized in a 28-byte grid as shown in Table 1.

Table 1. Content of the node data frame and its position in bytes

Bytes	Content
1	Node information
2	Node calibration
3–8	Accelerometer data (x, y and z axes)
9–14	Magnetometer data (x, y and z axes)
15–20	Gyroscope data (x, y and z axes)
21–28	Quaternion (x, y, z and w components)

Data flow. When a user initiates a physical therapy session, the proposed application starts reading all acquired data through the serial port of the smartphone or PC. This data acquisition is executed in parallel through a dedicated thread. In each loop, this application waits until it receives 210 bytes, comprised of 30 bytes of data from each of the seven sensor nodes. The first 210 bytes are taken as the initial condition of acquisition. In each of the seven nodes, the application obtains data such as node status, calibration information, angular acceleration, angular velocity, magnetic field, and orientation data. Based on an identification number found in each subframe, the application assigns this subframe to a lower limb segment.

Calibration of the sensor placement. Based on kinesiological conventions reported in [39], the articular angles of a patient in the anatomical position are zero. Therefore, the coordinate system of each sensor node of the lower limb segments is aligned with the vertical axis, as shown in Figure 5.

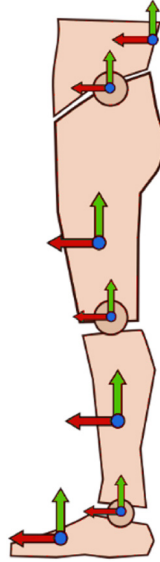


Fig. 5. Execution of the supervision

To initialize the lower limbs monitoring system, a patient must be in an anatomical position. In this condition, the quaternion of the initial orientation q_0 is calculated. Using this initial calibration, node orientation with respect to the anatomical position can be calculated accurately, despite registering deviations in the location of the nodes.

The node calibration process begins when the user checks the status of the nodes and verifies that all nodes are online. If the nodes are connected and calibrated correctly, a green checkbox is displayed and the session can be started. But if the checkboxes of the nodes are red, the system has a connection or calibration problem. To fix this problem, it is recommended to check the connections and reboot the system.

Based on [19], q_0 is defined with respect to the coordinate system of the hip node, which is the reference node. The z axis of the hip node coordinate system z_{hip} can be calculated as follows:

$$z_{hip} = [0_{3 \times 1} \quad I_{3 \times 3}] [q_{hip}^* \otimes [0 \quad z_0]^T \otimes q_{hip}] \quad (1)$$

where \otimes is the quaternion product, $z_0 = [0 \ 0 \ 1]^T$ is an orthogonal vector, orthogonal to the transversal plane and pointing upward, $0_{3 \times 1}$ is a matrix filled with zeros, $I_{3 \times 3}$ is the identity matrix, q_0 is the quaternion orientation of the hip node, and q_{hip}^* is its conjugate.

The projection of z_0 on the transversal plane is defined as

$$z_{hip-trans} = z_{hip} - [[z_{hip} \cdot z_0] \cdot z_0], \quad (2)$$

where \cdot is the dot product.

The forward direction of the patient x_p is then calculated as a normalized vector with opposite direction to $z_{hip-trans}$. Thus, the angle θ_x between the vector x_p and the global axis $x_0 = [1 \ 0 \ 0]^T$ is set as

$$\theta_x = \tan^{-1} \left[\frac{x_p \cdot x_0}{z_0 \cdot (x_0 \times x_p)} \right], \quad (3)$$

where \times is the cross-product. Then, the initial orientation quaternion is defined as

$$q_0 = \cos(\theta_x / 2) + \sin(\theta_x / 2) \cdot z_0. \quad (4)$$

Finally, the segment quaternions q_{seg} estimated by the IMU is rotated according to the sensor nodes' initial position. Thus, each calibrated segment quaternion q_{cal} is set as:

$$q_{cal} = q_{seg}^* \otimes q_0. \quad (5)$$

The linear acceleration a_{lin} of each segment is then obtained by rotating the acceleration vector a_{seg} around q_{cal} and subtracting the value of gravity on the z axis as

$$a_{lin} = (q_{cal} \cdot a_{seg}) - [0 \ 0 \ g]^T \quad (6)$$

Where g is 9.807 m/s^2 .

The quaternions of the lower limb joint deviations q_{joint} are calculated based on the quaternions of the distal and proximal segment, q_{prox} and q_{dist} , being the nearest and the furthest segment to the trunk respectively, then:

$$q_{joint} = q_{dist} \otimes q'_{prox}. \quad (7)$$

3 Results and discussion

In this section, the designed wearable virtual reality system for lower limb monitoring is tested to check its performance and evaluate its accuracy. The orientation angles measured by the inertial sensors are compared with the angles measured with a rotatory optical encoder and the motion analysis software Kinovea. The rotatory encoder has 3600 pulses per revolution with a resolution of 0.1° [40], and it is used here as a measurement pattern. The Kinovea software has been used as a benchmark in multiple projects [41]–[43].

3.1 Sensor validation

A pendulum is used to validate the functional behavior of the wearable virtual reality system for lower limb monitoring. Figure 6 shows the experiment developed, which includes the measurement pattern sensor (rotary encoder: OMRON E6D-C 3600 PPR) which is attached to the rotation axis of the pendulum. Two sensor nodes are used to test the system: one located on the end of the pendulum and the other on the chassis supporting the pendulum. The sensor node is located according to the anatomical planes previously defined. The two sensor nodes in their initial positions form a 90° angle. To compare the measurements made by the inertial sensors with the video analysis software Kinovea, a digital 13-megapixel camera with an $f/2.4$, $1/3''$ sensor size and a 1.12μ pixel size camera, $1080 p$ resolution and a frame rate of $30 fps$ are used. The camera is placed on a tripod, perpendicular to the pendulum's plane of rotation at a distance of $0.47 m$ and a height of $0.93 m$ above the floor. To measure the three rotational degrees of freedom (on the sagittal, frontal, and transverse planes), the sensor nodes are manually rotated to position the line of gravity along the axial planes.



Fig. 6. Experimental setup

To start the experiment, the end of the pendulum is placed at an angle of 90° with respect to the vertical and the pendulum is released. The pendulum angle is measured with the encoder, sensor nodes 1 and 2 and the video camera. Figure 7 shows the signal value generated by the encoder, the sensor node, and Kinovea. It also shows the error between the encoder and sensor node, and the error between the encoder and Kinovea for the sagittal plane. Figure 8 shows an enlargement of the signals that are shown in Figure 7 during the first 1.5 seconds. Similar figures were made for the frontal and transverse planes but are not shown here for the sake of brevity.

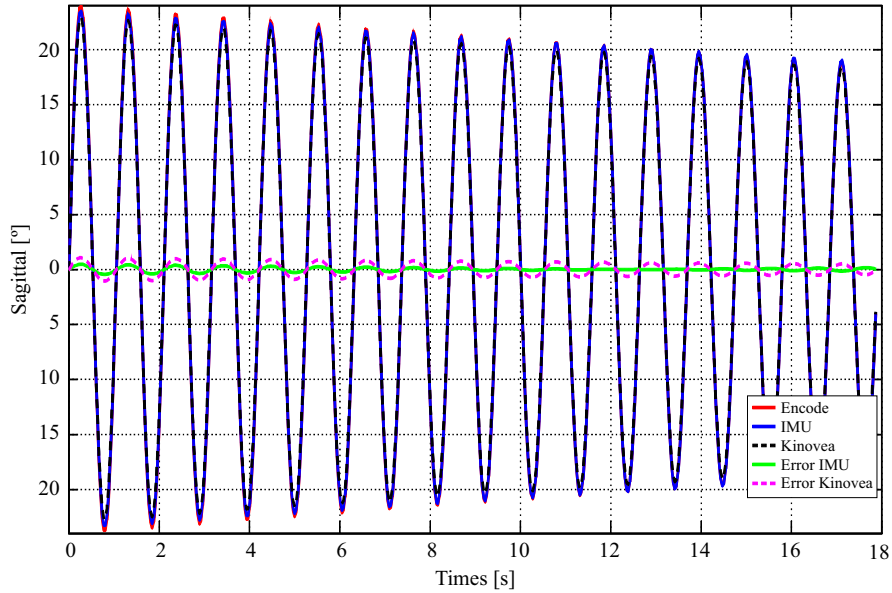


Fig. 7. Angles and errors in the sagittal plane

The maximum sensor node error is defined as the maximum error between the encoder and the sensor node divided by the maximum encoder amplitude during the experiment. The maximum Kinovea error is defined as the maximum error between the encoder and Kinovea divided by the maximum encoder amplitude during the experiment. Table 2 shows the maximum sensor node error and the maximum Kinovea error with respect to the pattern sensor (rotatory encoder) during the experimental evaluation. Errors are computed for sagittal, frontal, and transverse planes.

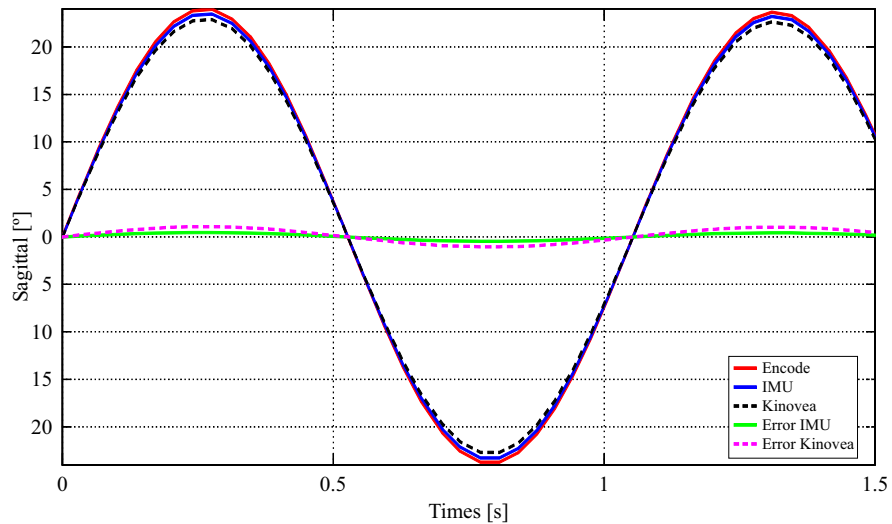


Fig. 8. Enlargement of the angles and errors in the sagittal plane

Table 2. Maximum error between the encoder and sensor node, and encoder and kinovea

	Sagittal %	Frontal %	Transverse %
Sensor node error	1.989	2.339	1.879
Kinovea error	4.465	0.644	1.894

As can be seen in Table 2, the maximum sensor node error is less than the maximum Kinovea error in the sagittal plane while the maximum sensor node error is larger than the maximum Kinovea error in the frontal plane. In the transverse plane, the maximum sensor node error is similar to the maximum Kinovea error. Measurements made using Kinovea’s software have greater error dispersion. This dispersion is associated with the camera calibration process and the manual processing of images during the marker tracking process.

To analyze the error behavior of the sensor nodes and Kinovea, a histogram is plotted for the transverse plane from the total experimental data, as shown in Figure 9. Similar figures have been obtained for sagittal and frontal planes but are not shown here for the sake of brevity. Using the error information from Figure 9, the standard deviation of sensor node error and Kinovea error for the sagittal, frontal and transverse planes are computed, as shown in Table 3. The mean of sensor node error and Kinovea error are zero, which shows that both measurement systems are unbiased.

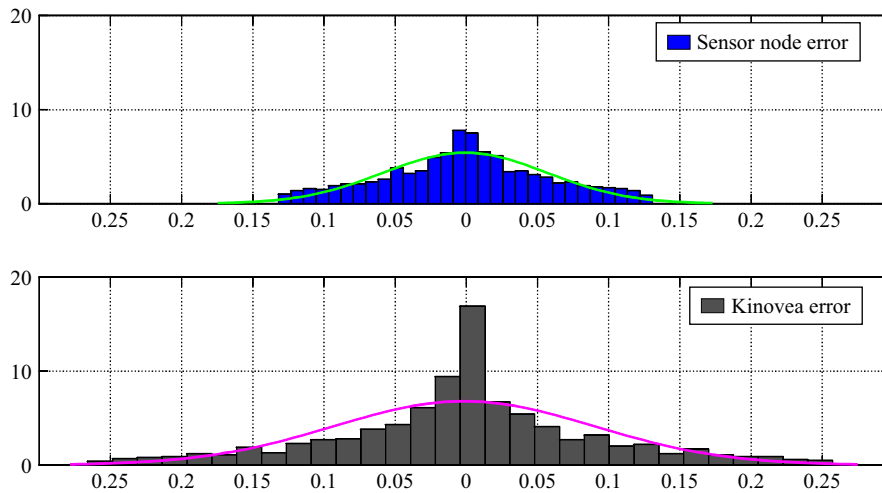


Fig. 9. Histogram of error signals for transverse plane

Table 3. Standard deviation of error signals for the sagittal, frontal and transverse planes

	Sagittal	Frontal	Transverse
Sensor node error	0.003	0.007	0.002
Kinovea error	0.012	0.002	0.003

As can be seen in Table 3, the standard deviation of sensor node error is less than the standard deviation of Kinovea error in the sagittal plane while the standard deviation of sensor node error is larger than the standard deviation of Kinovea error in the frontal plane. In the transverse plane, the standard deviation of sensor node error is similar to the standard deviation of Kinovea error. The means calculated for both sensor node error and Kinovea error are zero.

In general, it is possible to conclude that the maximum errors estimated by the system's sensor nodes are similar to those generated by using Kinovea. Our advantage is that the estimated data processing time through the sensor nodes is considerably less compared to the estimated data processing time needed by the Kinovea software. Furthermore, sensor nodes can be used anywhere with few tools required for data processing.

3.2 Supervision session test

For the supervision session test, the pelvis sensor node is placed on the patient's lower back, the thigh and leg sensor nodes are placed on the outer thighs and legs respectively, and the foot sensor nodes are placed on the upper part of each foot. The design of the sensor straps allows them to adapt to the contours of the limbs of the human body, in a comfortable and practical way, without affecting blood flow or joint movements. The sensor straps are adjustable, with a width of 5 cm and a length suitable for each limb contour. The material used in the straps is elastic and Velcro. The sensors are calibrated each time they are turned on or a new exercise session is started. The location of the sensor nodes on the patient is shown in Figure 10b and the method for angle measurement is shown in Figure 10a.



Fig. 10. Set of two subfigures of the location of the sensor nodes on the patient

The master node's processing time to acquire data from the seven nodes averages 9.67 ms and has a standard deviation of 0.056 ms. Drawing on information from the master node, which uses angular measurements from the seven sensor nodes, an avatar is set to move on a PC or smartphone display showing the patient's sagittal plane only. There is a 33 ms delay between the real body movement and that of the avatar. This delay is acceptable for visual feedback purposes since the human eye can perceive movements from images with a sampling time of 13 ms. The implemented virtual

reality system for lower limb monitoring ensures accurate measurement of the lower limbs' joint angles with low error magnitudes. Using an avatar as a visualization tool during physical therapy sessions is suitable for visual feedback purposes. After the user has performed an exercise session with the smartphone or PC, the final data will be available on the MySQL web server so that the user can visualize his progress or the specialist can view the user's evolution as many times as necessary, recreating the avatar's movements and the angular measurements of the lower limbs' joints.

4 Conclusion

In this paper, a system for human gait monitoring for lower limb rehabilitation has been developed. The system uses wireless wearable devices (inertial sensors), a smartphone or a PC, and software applications for data processing and on-site visual feedback by means of an avatar that recreates the movements of a patient's lower limbs. The developed system has seven sensor nodes which send information of joint angular changes from quaternions to a master node wirelessly. The developed system was validated using a high-resolution rotary encoder coupled to a pendulum as a reference or pattern. Experimental results show that the developed monitoring system has high accuracy, with maximum errors of 2% with respect to the maximum signal excursions in the transverse and sagittal planes, and 2.3% with respect to the maximum signal excursions in the frontal plane. If we compare the developed monitoring system and the Kinovea software with the pattern, the maximum error of the developed system in the sagittal plane is less than half the error obtained by the Kinovea software, while the maximum error of the developed system in the frontal plane is four times the error obtained by the Kinovea software, and the maximum error of the developed system in the transverse plane is similar to the error obtained by the Kinovea software. It is possible to conclude that the maximum errors estimated by the developed monitoring system are similar to those obtained by the Kinovea software. Our advantage is that the estimated data processing time through the sensor nodes is considerably less compared to the estimated data processing time needed by the Kinovea software. Furthermore, sensor nodes can be used anywhere with few tools required for data processing. The designed system uses a sampling rate of 10 ms with delays of 33 ms between the patient's body movement and the avatar's movement, being an acceptable delay for visual rehabilitation purposes. The developed system is portable and allows a patient to complete physiotherapy sessions at home or anywhere, with the advantage of allowing visual feedback through an avatar during on-site rehabilitation therapy. It also allows the physiotherapist to visualize the patient's progress as often as needed remotely on their PC or smartphone. This makes therapies more accessible to patients and enables an expert to create personalized therapy plans that can be reviewed online. Future work can include a gait evaluation with patients using the developed system and traditional systems.

Despite having a practical and useful monitoring system, there are limitations that could generate deviations of the kinematic variables, such as: the drift effect caused by some measured signals, which appear in cases of prolonged exercise sessions; or

inaccurate measurements due to incorrect grip of the sensor node on the patient's limb by the user; or the interference of magnetic fields that affect the measured signals, generating erroneous measurements. Additionally, the sensors require rechargeable batteries for their operation.

5 Acknowledgment

Edna Avella-Rodríguez thanks the project *Fortalecimiento de Capacidades del Talento Humano para la Educación y la Innovación Mediante Formación de Alto Nivel del Valle del Cauca – FAN No 121925*, and project CI.21145 of Universidad del Valle for its financial support.

6 References

- [1] M. Weerasinghe *et al.*, “Computer aid assessment of muscular imbalance for preventing overuse injuries in athletes,” in *ACM International Conference Proceeding Series*, 2016, pp. 244–248. <https://doi.org/10.1145/3018009.3018023>
- [2] H. K. Kim, S. A. Mirjalili, and J. Fernandez, “Gait kinetics, kinematics, spatiotemporal and foot plantar pressure alteration in response to long-distance running: Systematic review,” *Hum. Mov. Sci.*, vol. 57, pp. 342–356, 2018. <https://doi.org/10.1016/j.humov.2017.09.012>
- [3] V. Belluscio *et al.*, “Dynamic balance assessment during gait in children with Down and Prader-Willi syndromes using inertial sensors,” *Hum. Mov. Sci.*, vol. 63, pp. 53–61, 2019. <https://doi.org/10.1016/j.humov.2018.11.010>
- [4] M. Porta *et al.*, “Association between objectively measured physical activity and gait patterns in people with Parkinson's disease: Results from a 3-month monitoring,” *Parkinsons Dis.*, vol. 2018, pp. 1–10, 2018. <https://doi.org/10.1155/2018/7806574>
- [5] M. Ketcham, T. Ganokratanaa, and P. Pramkeaw, “Learning game with stroke paralysis rehabilitation for virtual reality,” *Int. J. Emerg. Technol. Learn.*, vol. 17, no. 21, pp. 38–74, 2022. <https://doi.org/10.3991/ijet.v17i21.34257>
- [6] S. S. Sabry, M. Sahib, and T. Nayl, “Toward hand functions rehabilitation using the virtual world for pre-school children with cerebral palsy,” *Int. J. Emerg. Technol. Learn.*, vol. 15, no. 09, p. 110, 2020. <https://doi.org/10.3991/ijet.v15i09.13047>
- [7] K. Frączkowski and S. Łaska, “Recognition of the Pathology of the Human Movement with the Use of Mobile Technology and Machine Learning,” in *Advances in Intelligent Systems and Computing*, vol. 833, Springer, Cham, 2019, pp. 533–541. https://doi.org/10.1007/978-3-319-98678-4_53
- [8] D. Jarchi, J. Pope, T. K. M. Lee, L. Tamjidi, A. Mirzaei, and S. Sanei, “A review on accelerometry-based gait analysis and emerging clinical applications,” *IEEE Rev. Biomed. Eng.*, vol. 11, pp. 177–194, 2018. <https://doi.org/10.1109/RBME.2018.2807182>
- [9] M. S. Tasjid and A. Al Marouf, “Leveraging smartphone sensors for detecting abnormal gait for smart wearable mobile technologies,” *Int. J. Interact. Mob. Technol.*, vol. 15, no. 24, pp. 167–175, 2021. <https://doi.org/10.3991/ijim.v15i24.25891>
- [10] K. A. Aljedaani and R. A. Alnanih, “Grounded theory for the design of mobile user interfaces-based on space retrieval therapy,” *Int. J. Interact. Mob. Technol.*, vol. 15, no. 12, p. 104, 2021. <https://doi.org/10.3991/ijim.v15i12.21487>

- [11] C. A. Collazos, H. E. Castellanos, J. A. Cardona, J. C. Lozano, A. Gutiérrez, and M. A. Riveros, “A Simple Physical Model of Human Gait Using Principles of Kinematics and BTS GAITLAB,” in *IFMBE Proceedings*, vol. 60, I. Torres, J. Bustamante, and D. A. Sierra, Eds. Singapore: Springer Singapore, 2017, pp. 333–336. https://doi.org/10.1007/978-981-10-4086-3_84
- [12] S. L. Colyer, M. Evans, D. P. Cosker, and A. I. T. Salo, “A review of the evolution of vision-based motion analysis and the integration of advanced computer vision methods towards developing a markerless system,” *Sport. Med. – Open*, vol. 4, no. 1, p. 24, 2018. <https://doi.org/10.1186/s40798-018-0139-y>
- [13] X. Xu, R. W. McGorry, L. S. Chou, J. hua Lin, and C. chi Chang, “Accuracy of the Microsoft Kinect™ for measuring gait parameters during treadmill walking,” *Gait Posture*, vol. 42, no. 2, pp. 145–151, 2015. <https://doi.org/10.1016/j.gaitpost.2015.05.002>
- [14] N. Jiang, L. Gizzi, N. Mrachacz-Kersting, K. Dremstrup, and D. Farina, “A brain-computer interface for single-trial detection of gait initiation from movement related cortical potentials,” *Clin. Neurophysiol.*, vol. 126, no. 1, pp. 154–159, 2015. <https://doi.org/10.1016/j.clinph.2014.05.003>
- [15] S. Arora *et al.*, “Detecting and monitoring the symptoms of Parkinson’s disease using smartphones: A pilot study,” *Parkinsonism Relat. Disord.*, vol. 21, no. 6, pp. 650–653, 2015. <https://doi.org/10.1016/j.parkreldis.2015.02.026>
- [16] T. Seel, J. Raisch, and T. Schauer, “IMU-based joint angle measurement for gait analysis,” *Sensors (Switzerland)*, vol. 14, no. 4, pp. 6891–6909, 2014. <https://doi.org/10.3390/s140406891>
- [17] W. Tao, T. Liu, R. Zheng, and H. Feng, “Gait analysis using wearable sensors,” *Sensors*, vol. 12, no. 2, pp. 2255–2283, 2012. <https://doi.org/10.3390/s120202255>
- [18] L. Vargas, A. Elias, A. Frizera, and E. Rocon, “Body to Sensor Calibration Procedure for Lower Limb Joint Angle Estimation Applied to Imu-Based Gait Analysis,” in *Proceedings of XXIV Brazilian Congress of Biomedical Engineering*, 2014, pp. 777–780.
- [19] L. S. Vargas-Valencia, A. Elias, E. Rocon, T. Bastos-Filho, and A. Frizera, “An IMU-to-body alignment method applied to human gait analysis,” *Sensors (Switzerland)*, vol. 16, no. 12, p. 2090, 2016. <https://doi.org/10.3390/s16122090>
- [20] Y. Zheng, K. C. Chan, and C. C. L. Wang, “Pedalvatar: An IMU-based real-time body motion capture system using foot rooted kinematic model,” in *IEEE International Conference on Intelligent Robots and Systems*, 2014, pp. 4130–4135. <https://doi.org/10.1109/IROS.2014.6943144>
- [21] V. Joukov, V. Bonnet, M. Karg, G. Venture, and D. Kulić, “Rhythmic extended Kalman filter for gait rehabilitation motion estimation and segmentation,” *IEEE Trans. Neural Syst. Rehabil. Eng.*, vol. 26, no. 2, pp. 407–418, 2018. <https://doi.org/10.1109/TNSRE.2017.2659730>
- [22] J. B. Lee, R. B. Mellifont, and B. J. Burkett, “The use of a single inertial sensor to identify stride, step, and stance durations of running gait,” *J. Sci. Med. Sport*, vol. 13, no. 2, pp. 270–273, 2010. <https://doi.org/10.1016/j.jsams.2009.01.005>
- [23] F. Hoflinger, J. Muller, R. Zhang, L. M. Reindl, and W. Burgard, “A wireless micro inertial measurement unit (IMU),” *IEEE Trans. Instrum. Meas.*, vol. 62, no. 9, pp. 2583–2595, 2013. <https://doi.org/10.1109/TIM.2013.2255977>
- [24] G. Li, T. Liu, L. Gu, Y. Inoue, H. Ning, and M. Han, “Wearable gait analysis system for ambulatory measurement of kinematics and kinetics,” in *Proceedings of IEEE Sensors*, 2014, vol. 2014 pp. 1316–1319. <https://doi.org/10.1109/ICSENS.2014.6985253>
- [25] J. Manit and P. Youngkong, “TailGait: A light-weight wearable gait analysis system,” in *Proceedings of the International Conference on Sensing Technology, ICST*, 2013, pp. 540–544. <https://doi.org/10.1109/ICSensT.2013.6727711>

- [26] N. Mathur, G. Paul, J. Irvine, M. Abuhelala, A. Buis, and I. Glesk, "A practical design and implementation of a low cost platform for remote monitoring of lower limb health of amputees in the developing world," *IEEE Access*, vol. 4, no. 99, pp. 7440–7451, 2016. <https://doi.org/10.1109/ACCESS.2016.2622163>
- [27] Y. Zhang, Y. Fei, L. Xu, and G. Sun, "Micro-IMU-based motion tracking system for virtual training," in *Chinese Control Conference, CCC*, 2015, vol. 2015-Sept, pp. 7753–7758. <https://doi.org/10.1109/ChiCC.2015.7260871>
- [28] I. Carpinella *et al.*, "Wearable sensor-based biofeedback training for balance and gait in Parkinson disease: A pilot randomized controlled trial," *Arch. Phys. Med. Rehabil.*, vol. 98, no. 4, pp. 622–630.e3, 2017. <https://doi.org/10.1016/j.apmr.2016.11.003>
- [29] J. C. Alcaraz, S. Moghaddamnia, and J. Peissig, "An Android-based application for digital gait performance analysis and rehabilitation," in *2015 17th International Conference on E-health Networking, Application & Services (HealthCom)*, 2015, pp. 640–643. <https://doi.org/10.1109/HealthCom.2015.7454582>
- [30] P. Aqueveque, S. Sobarzo, F. Saavedra, C. Maldonado, and B. Gómez, "Android platform for realtime gait tracking using inertial measurement units," *Eur. J. Transl. Myol.*, vol. 26, no. 3, p. 6144, 2016. <https://doi.org/10.4081/ejtm.2016.6144>
- [31] S. Nishiguchi *et al.*, "Reliability and validity of gait analysis by android-based smartphone," *Telemed. e-Health*, vol. 18, no. 4, pp. 292–296, 2012. <https://doi.org/10.1089/tmj.2011.0132>
- [32] J. S. Grover and V. Natarajan, "Estimation and tracking of knee angle trajectory using inertial sensors and a smartphone application," in *BodyNets International Conference on Body Area Networks*, 2015, pp. 1–7. <https://doi.org/10.4108/eai.28-9-2015.2261468>
- [33] S. Kumar, K. Gopinath, L. Rocchi, P. T. Sukumar, S. Kulkarni, and J. Sampath, "Towards a portable human gait analysis & monitoring system," in *2018 International Conference on Signals and Systems, ICSIGSYS 2018 – Proceedings*, 2018, pp. 174–180. <https://doi.org/10.1109/ICSIGSYS.2018.8372660>
- [34] R. Nussbaum, C. Kelly, E. Quinby, A. Mac, B. Parmanto, and B. E. Dicianno, "Systematic review of mobile health applications in rehabilitation," *Arch. Phys. Med. Rehabil.*, vol. 100, no. 1, pp. 115–127, 2019. <https://doi.org/10.1016/j.apmr.2018.07.439>
- [35] S. R. Bethi, A. RajKumar, F. Vulpi, P. Raghavan, and V. Kapila, "Wearable Inertial Sensors for Exergames and Rehabilitation," in *2020 42nd Annual International Conference of the IEEE Engineering in Medicine & Biology Society (EMBC)*, 2020, pp. 4579–4582. <https://doi.org/10.1109/EMBC44109.2020.9175428>
- [36] A. Rajkumar, F. Vulpi, S. R. Bethi, P. Raghavan, and V. Kapila, "Usability study of wearable inertial sensors for exergames (WISE) for movement assessment and exercise," *mHealth*, vol. 7, pp. 4–4, 2021. <https://doi.org/10.21037/mhealth-19-199>
- [37] Y. T. Tsai, W. Y. Jhu, C. C. Chen, C. H. Kao, and C. Y. Chen, "Unity game engine: Interactive software design using digital glove for virtual reality baseball pitch training," *Microsyst. Technol.*, Jan. 2019. <https://doi.org/10.1007/s00542-019-04302-9>
- [38] M. Smith, A. Maiti, A. D. Maxwell, and A. A. Kist, "Using Unity 3D as the Augmented Reality Framework for Remote Access Laboratories," in *Lecture Notes in Networks and Systems*, vol. 47, Springer, Cham, 2019, pp. 581–590. https://doi.org/10.1007/978-3-319-95678-7_64
- [39] R.T. Floyd, *Manual of Structural Kinesiology*, 20th ed. New York, 2018.
- [40] OMRON Corporation Industrial Automation Company, "Rotary Encoder E6B2-C, Datasheet." pp. 1–5, 2017.
- [41] A. M. El-Sayed, N. A. Hamzaid, K. Y. S. Tan, and N. A. Abu Osman, "Detection of prosthetic knee movement phases via in-socket sensors: A feasibility study," *Sci. World J.*, vol. 2015, 2015. <https://doi.org/10.1155/2015/923286>
- [42] B. H. Groh, T. Cibis, R. O. Schill, and B. M. Eskofier, "IMU-based pose determination of scuba divers' bodies and shanks," *2015 IEEE 12th Int. Conf. Wearable Implant. Body Sens. Networks, BSN 2015*, 2015. <https://doi.org/10.1109/BSN.2015.7299376>

- [43] C. Damsted, R. O. Nielsen, and L. H. Larsen, “Reliability of video-based quantification of the knee- and hip angle at foot strike during running,” *Int. J. Sports Phys. Ther.*, vol. 10, no. 2, pp. 147–54, 2015.

7 Authors

Alejandro Astudillo received his B.Sc. degree in Electronics Engineering and his M.Sc. degree in Automation Engineering from Universidad del Valle, Colombia, in 2015 and 2017, respectively. He joined the MECO Research Team at KU Leuven as a PhD researcher in 2018. His research interests focus on strategies for reducing the engineering effort and the computational burden of real time motion planning and model predictive control of robotic and complex mechatronic systems (email: alejandro.astudillovigoya@kuleuven.be).

Edna Avella-Rodríguez received her degree in Electronics Engineering (2010) from Universidad Pedagógica y Tecnológica de Colombia, Colombia, and her M.Sc. degree in Automation Engineering (2016) from Universidad del Valle, Colombia. She is currently a PhD student at Universidad del Valle. Her research interests focus on technology control applications and biological control systems (email: edna.avella@correounivalle.edu.co).

Gloria Arango-Hoyos received her degree in Physiotherapy (1989) from Universidad del Valle, Colombia, and her M.Sc. degree in Neurorehabilitation (2013) from Universidad Autónoma de Manizales. She has been a professor since 1996 at Universidad del Valle. Her research interest focuses on health-related biotechnology (email: gloria.arango@correounivalle.edu.co).

Jose Ramirez-Scarpetta Electrical Engineer (1986), Master in Energy Generation Systems (1989) from the Universidad del Valle, Colombia; DEA (1994) and Ph.D. (1998) in Control Systems from the Polytechnic National Institute of Grenoble, France. Professor since 1988 at Universidad del Valle. Pre and postgraduate teaching in mathematical modeling, control systems and electromechanical drives. Research fields: optimal and non-linear control, engineering education (email: jose.ramirez@correounivalle.edu.co).

Esteban Rosero received the B.Sc. degree in Mechanical Engineering and M.Sc. degree in Automation Engineering from Universidad del Valle, Colombia, in 2001 and 2006, respectively. He worked in Cenicaña from 2001 to 2002. From 2010 to 2014, he pursued his Ph.D. degree at the Institute of Control Systems at Hamburg University of Technology, Germany. He is currently an Assistant Professor with the School of Electrical and Electronics Engineering at Universidad del Valle in Cali, Colombia. His research interests include the modeling and control of dynamic systems, cooperative and autonomous systems, mobile robotics and industrial processes (email: esteban.rosero@correounivalle.edu.co).

Article submitted 2023-02-11. Resubmitted 2023-03-24. Final acceptance 2023-04-06. Final version published as submitted by the authors.